

Magnetic and calorimetric studies of anomalous Pr antiferromagnetic ordering in orthorhombic $\text{Pb}_2\text{Sr}_2\text{PrCu}_3\text{O}_8$

J. H. Shieh and H. C. Ku

Department of Physics, National Tsing Hua University, Hsinchu, Taiwan 300, Republic of China

J. C. Ho

Department of Physics, Wichita State University, Wichita, Kansas 67260

(Received 14 April 1994)

Magnetic measurements on vacuum-annealed orthorhombic $\text{Pb}_2\text{Sr}_2\text{PrCu}_3\text{O}_{8+y}$ ($y \approx 0$) reveal an anomalous Pr antiferromagnetic ordering at $T_N(\text{Pr}) \approx 6$ K with transition onset up to 11 K. This Pr-2213 compound shares common structural features with the tetragonal Pr-123 compound $\text{PrBa}_2\text{Cu}_3\text{O}_6$, which also undergoes a Pr ordering at 10 K. However, oxygenated pseudotetragonal $\text{Pb}_2\text{Sr}_2\text{PrCu}_3\text{O}_{8+y}$ ($y \approx 1$) exhibits only low transition onset around 3 K, while orthorhombic $\text{PrBa}_2\text{Cu}_3\text{O}_7$ has a higher $T_N(\text{Pr})$ value of 17 K. Complementary studies by adiabatic calorimetry on $\text{Pb}_2\text{Sr}_2\text{PrCu}_3\text{O}_8$ yield a specific-heat anomaly with a peak near the magnetically derived $T_N(\text{Pr})$, with onset around 11 K. A large heavy-fermion-like linear term in the specific heat prevails as often observed in other Pr-containing high- T_c systems. The magnetic entropy ΔS_m below 11 K onset is relatively small, only 13% of $R \ln 3$ for Pr^{3+} with a quasitriplet ground state, implying a quasi-2D nature of the magnetic ordering with a strong 2D short-range magnetic correlation which persists to higher temperatures in this extremely anisotropic structure.

I. INTRODUCTION

The anomalously high Pr antiferromagnetic ordering temperature of 17 K for $\text{PrBa}_2\text{Cu}_3\text{O}_7$, which happens to be the only nonsuperconducting member of the $R\text{Ba}_2\text{Cu}_3\text{O}_7$ (R -123) system ($R = \text{Y}$ or most rare earths), has been the focus of extensive research ever since the discovery of high- T_c superconductors.¹⁻³ With further oxygen deficiency, $T_N(\text{Pr})$ decreases to 10 K in $\text{PrBa}_2\text{Cu}_3\text{O}_6$.^{2,4} In comparison, other magnetic rare-earth compounds have a maximum $T_N(R)$ of 2.2 K in $\text{GdBa}_2\text{Cu}_3\text{O}_7$.^{5,6} Meanwhile, Pr substitution leads to T_c suppression from above 90 K in $(R_{1-x}\text{Pr}_x)\text{Ba}_2\text{Cu}_3\text{O}_7$. For $x > 0.5$, superconductivity is totally quenched, and Pr ordering begins to set in.² Similar anomalous Pr magnetic behavior has been observed in two- CuO_2 layer $\text{TlBa}_2\text{PrCu}_2\text{O}_7$ (Tl-1212) compound and related Pr-containing $\text{Tl}(\text{Ba},\text{Sr})_2\text{PrCu}_2\text{O}_7$ and $(\text{Pb},\text{Cu})\text{Sr}_2\text{PrCu}_2\text{O}_7$ systems,⁷⁻¹⁰ with the $T_N(\text{Pr})$ value ranges from 8 to 4 K. However, no Pr anomaly was observed for another two- CuO_2 layer compound $\text{Bi}_2\text{Sr}_2\text{PrCu}_2\text{O}_8$ (Bi-2212) down to 1.6 K.¹¹ Various types of experiments have been performed to substantiate these anomalous Pr phenomena in the Pr-123 and Pr-1212 systems and to clarify the mechanism of magnetic order and/or superconductivity suppression, but a clear picture is still elusive. Obviously, additional information from more diverse systems would be extremely helpful toward delineating the various factors which may play critical roles in this regard. This work was, therefore, carried out on the two- CuO_2 layer Pr system $\text{Pb}_2\text{Sr}_2\text{PrCu}_3\text{O}_{8+y}$ ($y \approx 0$ and 1). These Pr compounds belong to the $\text{Pb}_2\text{Sr}_2(R,\text{Ca})\text{Cu}_3\text{O}_{8+y}$ (Pb-2213) family ($R = \text{Y}$ or rare earths; $0 \leq y \leq 1.5$), where

stable superconductivity in the range 70 K was reported.^{12,13} For the Ca-free $\text{Pb}_2\text{Sr}_2\text{RCu}_3\text{O}_{8+y}$ system, no bulk superconductivity was observed, although filamentary superconductivity or superconductinglike resistivity drop around 70 K was reported for most of the vacuum-annealed samples.^{12,14}

II. EXPERIMENTS

The $\text{Pb}_2\text{Sr}_2\text{PrCu}_3\text{O}_{8+y}$ sample was prepared by two-stage solid-state reaction techniques. High-purity SrCO_3 , Pr_2O_3 , and CuO powders with the ratio $\text{Sr}:\text{Pr}:\text{Cu} = 2:1:3$ were well mixed, grounded and calcined at 930°C in air with at least one intermediate grinding. The precursor $\text{Sr}_2\text{PrCu}_3\text{O}_x$ powders were then mixed with the appropriate amounts of PbO , heated at 750°C in air for 12 h with intermediate grindings. For vacuum-annealed, oxygen-reduced samples ($y \approx 0$), the reacted powders were pressed into pellets and annealed at 870°C in vacuum (about 10^{-2} torr) for 24 h followed by furnace cooling. For oxygen-annealed samples ($y \approx 1$), the vacuum-reacted pellets were again put at 400°C in flowing oxygen for 48 h followed by furnace cooling. Other oxygen-reduced rare-earth compounds $\text{Pb}_2\text{Sr}_2\text{RCu}_3\text{O}_8$ ($R = \text{Y}, \text{Nd}, \text{Sm}, \text{Eu}, \text{Gd}, \text{Dy}, \text{and Ho}$) were prepared using the same method.

Structure analysis was made by a Rigaku Rotaflex rotating anode powder x-ray diffractometer using $\text{Cu } K\alpha$ radiation with a scanning rate of 0.5° in 2θ per minute. A Lazy Pulveriz-PC program (version 1) was employed for phase identifications and lattice parameter calculations. Ac electrical resistivity measurements (16 Hz) were carried out by the standard four-probe method with

a stable rms current of $3 \mu\text{A}$ down to 30 K in a closed-cycle refrigerator. dc magnetic susceptibility measurements were made with a Quantum Design MPMS superconducting quantum interference device magnetometer from 2 to 350 K with applied magnetic fields up to 1 T. Low-field ac magnetic susceptibility measurements were made with a Lake Shore 7221 susceptometer and/or magnetometer from 4.2 to 300 K with low rms magnetic fields from 0.005 up to 1 G in the frequency range of 100–1000 Hz. Specific-heat data were obtained by an adiabatic calorimeter for the temperature range of 2 to 14 K, with Joule heating and germanium thermometry.

III. RESULTS AND DISCUSSION

The powder x-ray-diffraction patterns of the vacuum-annealed $\text{Pb}_2\text{Sr}_2\text{PrCu}_3\text{O}_{8+y}$ ($y \approx 0$) Pr-2213 sample is shown in Fig. 1. The orthorhombic splitting of the $(20l/02l)$ ($l=0$ and 1) diffraction lines for this oxygen-reduced compound are more clearly shown in Fig. 2, with lattice parameters $a = 5.454(2) \text{ \AA}$, $b = 5.486(2) \text{ \AA}$, $c = 15.823(6) \text{ \AA}$, and unit-cell volume $V = 473.4(2) \text{ \AA}^3$. This orthorhombic structure with space group $Cmmm$ (Refs. 12 and 15) is very similar to that of the tetragonal Pr-123 $\text{PrBa}_2\text{Cu}_3\text{O}_6$ ($a = 3.898 \text{ \AA}$, $c = 11.84 \text{ \AA}$, and space group $P4/mmm$).⁴ The schematic comparison between these two structures are shown in Fig. 3, where a pseudotetragonal lattice parameter of $a_t = (a^2 + b^2)^{0.5} / 2 = 3.868 \text{ \AA}$ is used for $\text{Pb}_2\text{Sr}_2\text{PrCu}_3\text{O}_8$. The main difference from $\text{PrBa}_2\text{Cu}_3\text{O}_6$ is the replacement of the lone Cu plane by PbO-Cu-PbO planes (the Pb_2CuO_2 block module). The origin of the orthorhombic distortion is due to the nonequivalent $16(r)$ O(2) positions of oxygen atoms in the PbO layers. Because of the lone pairs of electrons of the Pb^{2+} cations, two basal O(2) oxygen atoms of the pyramid surrounding Pb^{2+} move closer to the cation while the other two move further away.¹⁵ The oxygen parameter $y \approx 0$ is confirmed by the powder-neutron-diffraction Rietveld analysis.¹⁶

Upon annealing the oxygen-reduced sample in flowing oxygen at 400°C for 2 days, the oxidized sample of

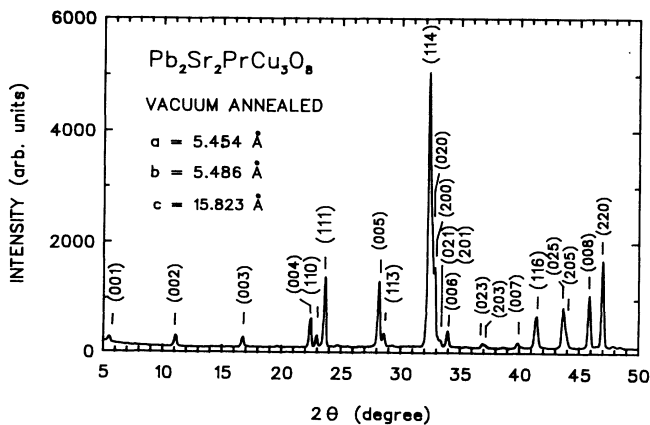


FIG. 1. Powder x-ray-diffraction patterns of the vacuum-annealed $\text{Pb}_2\text{Sr}_2\text{PrCu}_3\text{O}_{8+y}$ ($y \approx 0$) Pr-2213 orthorhombic sample ($a = 5.454 \text{ \AA}$, $b = 5.486 \text{ \AA}$, $c = 15.823 \text{ \AA}$).

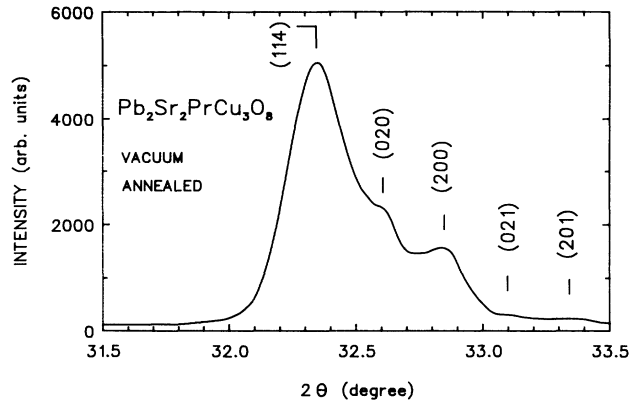


FIG. 2. The orthorhombic splitting of $(20l/02l)$ ($l=0$ and 1) diffraction lines for the vacuum-annealed $\text{Pb}_2\text{Sr}_2\text{PrCu}_3\text{O}_8$ sample

$\text{Pb}_2\text{Sr}_2\text{PrCu}_3\text{O}_{8+y}$ ($y \approx 1$) remains slightly orthorhombic with lattice parameters $a = 5.507(2) \text{ \AA}$, $b = 5.510(2) \text{ \AA}$, $c = 15.881(6) \text{ \AA}$ and a larger unit-cell volume V of $481.9(2) \text{ \AA}^3$. The splitting between the $(20l/02l)$ diffraction lines for this pseudotetragonal sample shown in Fig. 4 is barely observable, indicates the closeness of this sample to the orthorhombic-tetragonal transition boundary where the isostructural $\text{Pb}_2\text{Sr}_2\text{YCu}_3\text{O}_{8+y}$ system show such a transition around $y \approx 1$.^{17,18} The extra oxygen atoms are intercalated into the Cu layer sandwiched between two PbO layers.^{17,18}

Both samples ($y \approx 0$ and 1) show semiconducting behavior down to 30 K from ac electrical resistivity measurements. However, the vacuum-annealed samples ($y \approx 0$) give a low-room-temperature resistivity $\rho(\text{RT})$ of $530 \text{ m}\Omega \text{ cm}$ and some samples show filamentary diamagnetic signals ($< 1\%$) below 60 K in very low field ($< 1 \text{ G}$) ac magnetic susceptibility measurements.¹⁶

The variation of orthorhombic unit-cell volume for the oxygen-reduced $\text{Pb}_2\text{Sr}_2\text{RCu}_3\text{O}_8$ samples ($R = \text{Pr, Nd}$,

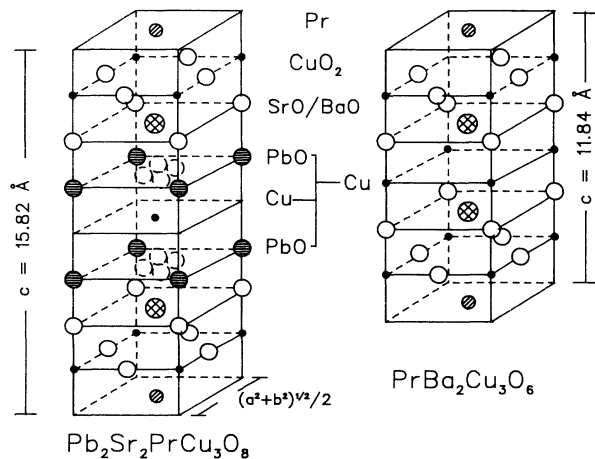


FIG. 3. A schematic comparison between the structures of tetragonal $\text{PrBa}_2\text{Cu}_3\text{O}_6$ ($P4/mmm$) and orthorhombic $\text{Pb}_2\text{Sr}_2\text{PrCu}_3\text{O}_8$ ($Cmmm$).

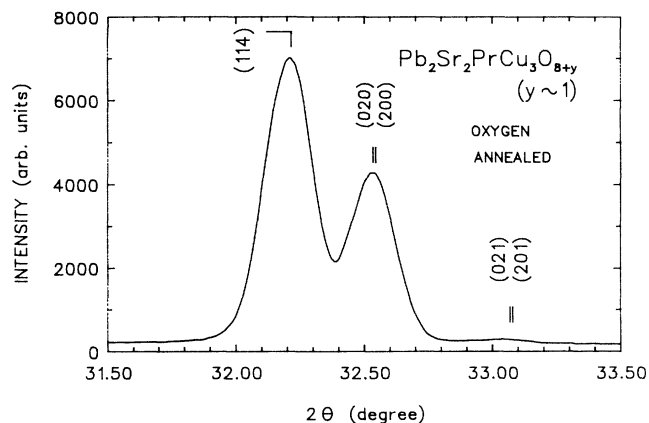


FIG. 4. The much reduced splitting of orthorhombic (201/021) diffraction lines for the oxygen-annealed $\text{Pb}_2\text{Sr}_2\text{PrCu}_3\text{O}_{8+y}$ ($y \approx 1$) pseudotetragonal sample ($a = 5.507$ Å, $b = 55.10$ Å, $c = 15.881$ Å).

Sm, Eu, Gd, Dy, Ho, and Y) with respect to the R^{3+} ionic radius as plotted in Fig. 5 followed a common linear line indicates the Pr^{3+} nature in $\text{Pb}_2\text{Sr}_2\text{PrCu}_3\text{O}_8$. The deviation of the Pr^{4+} point is as shown for comparison.

The temperature dependence of molar magnetic susceptibility χ_m of the vacuum-annealed $\text{Pb}_2\text{Sr}_2\text{PrCu}_3\text{O}_8$ sample in a 1-T applied magnetic field is shown in Fig. 6. Small fluctuation observed above room temperature indicates a possible Cu^{2+} magnetic ordering around or above 350 K. High applied field of 1 T is used in order to suppress the possible magnetic coupling between the Cu^{2+} moments and the Pr^{3+} moments. A simple Curie-Weiss fit $\chi_m = C/(T + \theta_p)$ is obtained below 100 K from the low-temperature inverse magnetic susceptibility $\chi_m^{-1}(T)$ (Fig. 7), which yields a negative paramagnetic intercept $\theta_p = -10.1$ K and an effective magnetic moment of $2.78\mu_B$ per Pr if the small Cu^{2+} moment can be neglected. The effective moment observed seems to be closer to the free Pr^{4+} ($2.54\mu_B$) rather than

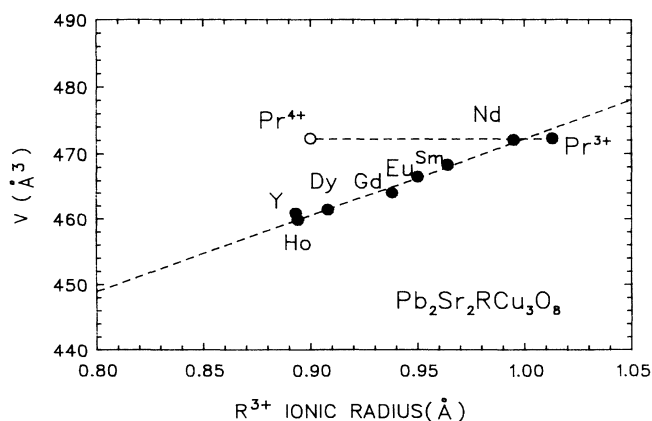


FIG. 5. Orthorhombic unit-cell volume V of the vacuum-annealed $\text{Pb}_2\text{Sr}_2\text{RCu}_3\text{O}_8$ compounds versus rare earth R^{3+} ionic radius and Pr^{4+} ionic radius.

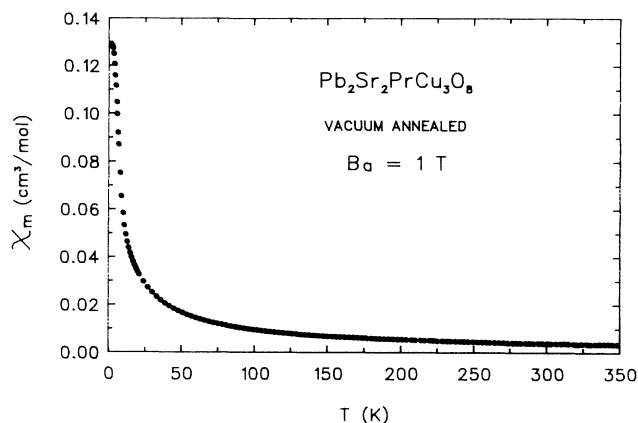


FIG. 6. Temperature dependence of molar magnetic susceptibility χ_m of vacuum-annealed $\text{Pb}_2\text{Sr}_2\text{PrCu}_3\text{O}_8$ in a 1-T applied magnetic field.

Pr^{3+} ($3.58\mu_B$). However, the magnetic measurements are always complicated by the crystal-field effect. Experimental evidence so far on Pr-containing high- T_c systems implies a Pr^{3+} state. For example, detailed crystal-field splitting schemes were obtained from inelastic neutron-scattering data based on Pr^{3+} in $\text{PrBa}_2\text{Cu}_3\text{O}_{7-y}$ with a quartet ground state, which can be used to derive a Curie-Weiss-like behavior and to generate the measured magnetic susceptibility.^{19,20} Considering the structural similarity, the same argument will likely be valid. Recently, Fehrenbacher and Rice²¹ proposed a more realistic picture, in which a Pr^{3+} ion is hybridized to the adjacent two CuO_2 layers. From such an orbital ($\text{Pr-}4f$ and $\text{O-}2p\pi$) overlap, Pr-Pr coupling can be greatly enhanced through a superexchange mechanism. The negative paramagnetic intercept of -10.1 K and the low-temperature deviation from the Curie-Weiss fit around 11 K or this vacuum-annealed $\text{Pb}_2\text{Sr}_2\text{PrCu}_3\text{O}_8$ sample indicate the occurrence of Pr long-range antiferromagnetic order. The exact T_N (Pr) value can be obtained from the low-temperature differential molar magnetic susceptibility $d\chi_m/dT$ as shown in Fig. 8. The transition occurs at

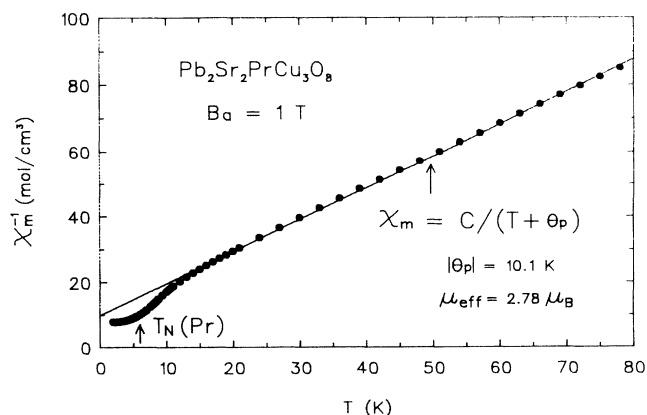


FIG. 7. Low-temperature inverse molar magnetic susceptibility χ_m^{-1} of $\text{Pb}_2\text{Sr}_2\text{PrCu}_3\text{O}_8$.

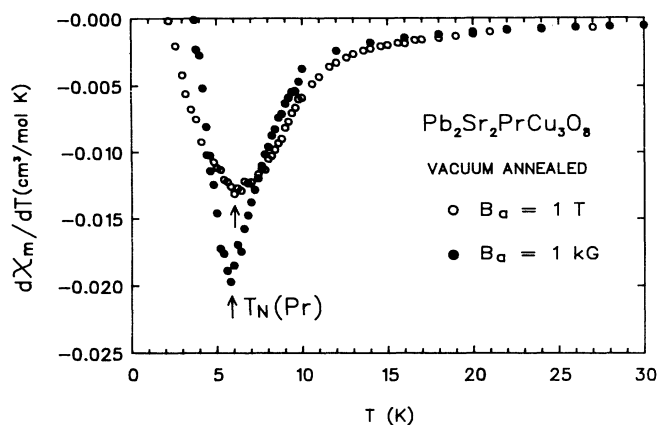


FIG. 8. Low-temperature differential molar magnetic susceptibility $d\chi_m/dT$ for the vacuum-annealed $\text{Pb}_2\text{Sr}_2\text{PrCu}_3\text{O}_8$ sample in two different applied fields of 1 kG and 1T.

5.8 K in a 1-kG field and 6 K in a 1-T field, judging from the minima of $d\chi_m/dT$. This value is much higher than the reported $T_N(\text{Gd}) = 2.3$ K in $\text{Pb}_2\text{Sr}_2\text{GdCu}_3\text{O}_8$.²²⁻²⁴

For the oxygen-annealed sample $\text{Pb}_2\text{Sr}_2\text{PrCu}_3\text{O}_{8+y}$ ($y \approx 1$), a much low negative paramagnetic intercept $\theta_p = -2.0$ K was observed from inverse magnetic susceptibility. The temperature dependence of $d\chi_m/dT$ presented in Fig. 9 shows no minimum down to 2 K. However, a deviation from the Curie-Weiss fit (solid line) indicates a possible Pr ordering onset around 3 K. There is clearly a significant dependence of $T_N(\text{Pr})$ on the oxygen content in the Pr-2213 system, but in a direction opposite to that in $\text{PrBa}_2\text{Cu}_3\text{O}_{7-y}$ (17 K for $y \approx 0$ and 10 K for $y \approx 1$). This needs to be taken into consideration toward a unified model to interpret Pr-Pr effective magnetic coupling based on the superexchange mechanism through hybridization between the extended Pr-4f wave function and O-2p π orbital of the adjacent two-CuO₂ layers. It is of interest to note

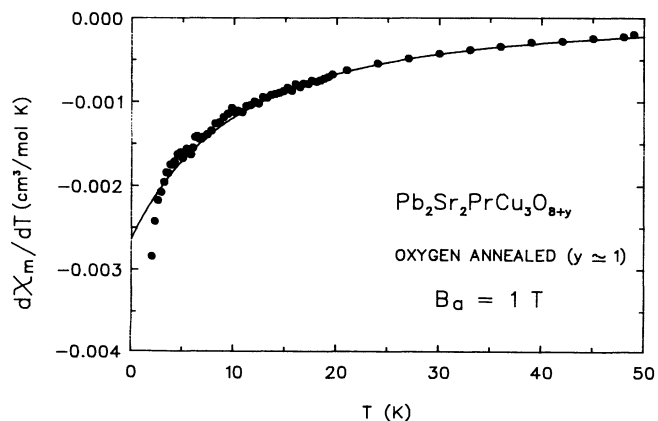


FIG. 9. Low-temperature differential molar magnetic susceptibility $d\chi_m/dT$ for the oxygen-annealed $\text{Pb}_2\text{Sr}_2\text{PrCu}_3\text{O}_{8+y}$ ($y \approx 1$) sample in a 1-T applied field. The Curie-Weiss fit is indicated by the solid line.

that, while the lattice parameters of the tetragonal $\text{Tl}(\text{Ba}_{1-x}\text{Sr}_x)_2\text{PrCu}_2\text{O}_7$ Pr-1212 system decrease as expected with increased Sr contents, the Pr-O bond length actually increases, yielding a reduction of $T_N(\text{Pr})$ from 8 K for $x=0$ to 4 K for $x=1$.¹⁰

To supplement the magnetic studies on Pr ordering in $\text{Pb}_2\text{Sr}_2\text{PrCu}_3\text{O}_8$, specific-heat measurements between 2 and 14 K were made. The data for the vacuum-annealed sample shown in Fig. 10 gives a broad anomaly below approximately 11 K (the same temperature where χ_m begins to deviate from the Curie-Weiss fit), reaching a peak near the magnetically derived $T_N(\text{Pr}) \approx 6$ K. It is possible that this $T_N(\text{Pr})$ represents the true three-dimensional or quasi-two-dimensional long-range magnetic ordering, above which the extra specific heat arises from 2D ordering effects with long-range 2D correlation below 11 K and fluctuating short-range correlation extended to much higher temperatures. The latter should be reflected in magnetic entropy consideration. To better illustrate it, the temperature dependence of C/T is shown in Fig. 11. The dashed line represents the sum of a large heavy-fermion-like linear term γT and a T^3 -dependent lattice contribution $C_1 = \beta T^3$ from the total specific heat. It is based on an extrapolation from higher-temperature data in a C/T vs T^2 plot shown in Fig. 12, where a large linear term coefficient γ of 200 mJ/mol K² and a Debye temperature θ_D of 280 K are derived. A relatively small magnetic entropy change $\Delta S_m = \int (C/T)dT \approx 1.1$ J/mol K is derived from the magnetic anomaly between 11 and 2 K, which is equal to 19% of $R \ln 2$ or 13% of $R \ln 3$ for Pr^{3+} with a quasitriplet ground state.^{19,20} Recent neutron-diffraction measurements indicate that the Pr magnetic ordering is an imperfect 3D (quasi-2D) ordering.¹⁶ The magnetic intensities observed at 1.4 K can be explained by assuming long-range ordering in the ab plane and a short-range correlation length of 20 Å along the c axis. The magnetic ordering is quasi-2D in nature in this highly anisotropic system where the Pr-Pr distance along the c axis of 15.8 Å is the longest distance for all Pr high- T_c systems, due to the existence of the long trilayer Pb_2CuO_2 block module.⁹ The basic magnetic

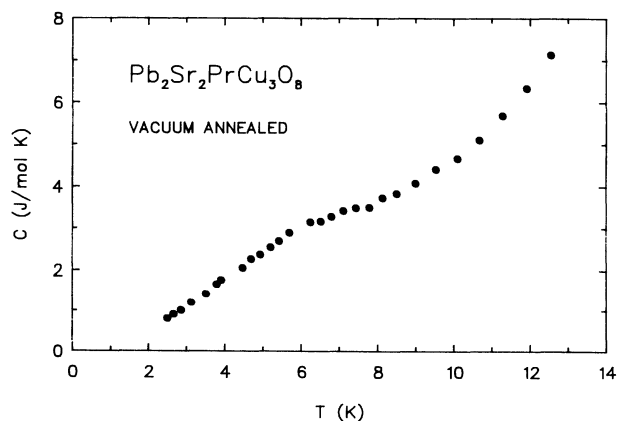


FIG. 10. Low-temperature molar specific heat C of vacuum-annealed $\text{Pb}_2\text{Sr}_2\text{PrCu}_3\text{O}_8$ with a Pr ordering onset around 11 K and a specific-heat peak at $T_N(\text{Pr}) = 6.0$ K.

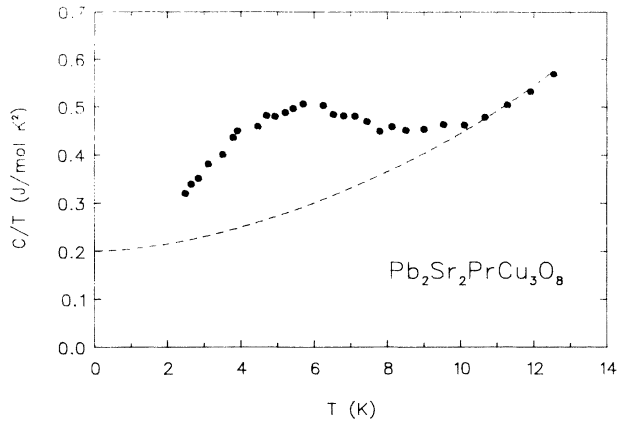


FIG. 11. C/T vs T of $\text{Pb}_2\text{Sr}_2\text{PrCu}_3\text{O}_8$ for entropy estimation. The dashed curve is taken from Fig. 12 (C/T versus T^2). The magnetic entropy change between 2 and 11 K is $\Delta S=1.1$ J/mol K^2 .

structure consists of the nearest-neighbor spins that are aligned antiparallel along all three crystallographic directions.¹⁶

The magnitude of magnetic entropy change ΔS_m seems to be closely related to the dimensionality of the magnetic order. In the more 3D-like Pr ordering in $\text{TlBa}_2\text{PrCu}_2\text{O}_7$ with $T_N(\text{Pr}) = 8$ K and onset at 10 K,^{7,8} a larger magnetic entropy change ΔS_m of 49% $R \ln 2$ or 31% of $R \ln 3$ was observed. The origin of the large linear term has not been fully understood yet. It is almost a common feature in all Pr-containing high- T_c systems. Its behavior below $T_N(\text{Pr})$ could affect significantly the magnetic entropy estimate. It is not unlikely that the coefficient of this linear term may drop gradually toward zero as temperature decreases, or even become quenched as soon as the ordering process sets in. Even so, the total magnetic entropy would still be less than $R \ln 3$ below 11 K, implying the

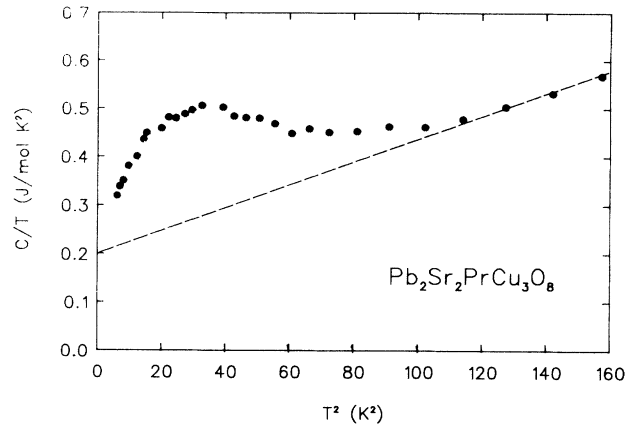


FIG. 12. C/T vs T^2 of $\text{Pb}_2\text{Sr}_2\text{PrCu}_3\text{O}_8$, with a large linear term coefficient γ of 200 mJ/mol K^2 .

presence of a 2D short-range magnetic correlation at higher temperatures. Such a phenomenon can be a consequence of the extremely anisotropic nature of high- T_c systems.

IV. CONCLUSION

In conclusion, this work on $\text{Pb}_2\text{Sr}_2\text{PrCu}_3\text{O}_{8+y}$ ($y \approx 0, 1$) compounds adds to the data base concerning many anomalous effects of antiferromagnetic Pr ordering in high- T_c systems.

ACKNOWLEDGMENTS

We thank Professor H. D. Yang and Professor W. H. Li for helpful discussions. The work was supported by the National Science Council of the Republic of China under Contract No. NSC83-0212-M007-069.

¹A. Kebede, C. S. Jee, J. Schwegler, J. E. Crow, T. Mihalisin, G. H. Myer, R. E. Salomon, P. Schlottmann, M. V. Kuric, S. H. Bloom, and R. P. Guertin, *Phys. Rev. B* **40**, 4453 (1989).

²H. B. Radousky, *J. Mater. Res.* **7**, 1917 (1992), and references cited therein.

³H. C. Ku, C. C. Chen, and S. W. Hsu, *Int. J. Mod. Phys. B* **2**, 1411 (1988).

⁴S. Uma, T. Sarker, M. Seshasayee, G. Rangarajan, C. R. Venkateswara Rao, and C. Subramanian, *Solid State Commun.* **87**, 289 (1993).

⁵J. C. Ho, P. H. Hor, R. L. Meng, C. W. Chu, and C. Y. Hung, *Solid State Commun.* **63**, 711 (1987).

⁶J. W. Lynn, in *High Temperature Superconductivity*, edited by J. W. Lynn (Springer-Verlag, Berlin, 1990), Chap. 8, p. 268, and references cited therein.

⁷C. C. Lai, B. S. Chiou, Y. Y. Chen, J. C. Ho, and H. C. Ku, *Physica C* **202**, 1004 (1992).

⁸W. T. Hsieh, K. J. Chang, W. H. Li, K. C. Lee, J. W. Lynn, C. C. Lai, and H. C. Ku, *Phys. Rev. B* **49**, 12200 (1994).

⁹H. C. Ku, C. C. Lai, J. H. Shieh, J. W. Liou, C. Y. Wu, and J. C. Ho, *Physica B* **194-196**, 223 (1994).

¹⁰C. C. Lai, T. J. Lee, H. K. Fun, H. C. Ku, and J. C. Ho, *Phys. Rev. B* (to be published).

¹¹Y. Gao, P. Perambuco-Wise, J. E. Crow, J. O'Reilly, H. Chen, and R. E. Salomon, *Phys. Rev. B* **45**, 7346 (1992).

¹²R. J. Cava, B. Batlogg, J. J. Krajewski, L. W. Rupp, Jr., L. F. Schneemeyer, T. Siegrist, R. B. van Dover, P. Marsh, W. F. Peck, Jr., P. K. Gallagher, S. H. Glarum, J. H. Marshall, R. C. Farrow, J. V. Waszczak, R. Hull, and P. Trevor, *Nature (London)* **336**, 211 (1988).

¹³M. A. Subramanian, J. Gopalakrishnan, C. C. Torardi, P. L. Gai, E. D. Boyes, T. R. Askew, R. B. Fippen, W. E. Farneth, and A. W. Sleight, *Physica C* **157**, 124 (1989).

¹⁴R. Prasad, N. C. Soni, K. Adhikary, S. K. Malik, and C. V. Tomy, *Solid State Commun.* **76**, 667 (1990).

¹⁵R. J. Cava, M. Marezio, J. J. Krajewski, W. F. Peck, Jr., A. Santoro, and F. Beech, *Physica C* **157**, 272 (1989).

¹⁶W. T. Hsieh, W. H. Li, K. C. Lee, J. W. Lynn, J. H. Shieh,

- and H. C. Ku, *J. Appl. Phys.* (to be published).
- ¹⁷M. Marezio, A. Santoro, J. J. Capponi, E. A. Hewat, R. J. Cava, and F. Beech, *Physica C* **169**, 401 (1990).
- ¹⁸M. Marezio, A. Santoro, J. J. Capponi, R. J. Cava, O. Chmaissem, and Q. Huang, *Physica C* **199**, 365 (1992).
- ¹⁹L. Soderholm, C. K. Loong, G. L. Goodman, and B. D. Dabrowski, *Phys. Rev. B* **43**, 7923 (1991).
- ²⁰G. Hilsher, E. Holland-Moritz, T. Holubar, H. D. Jostarndt, V. Nekvasil, G. Schaudy, U. Walter, and G. Fillion, *Phys. Rev. B* **49**, 535 (1994).
- ²¹R. Fehrenbacher and T. M. Rice, *Phys. Rev. Lett.* **70**, 3471 (1993).
- ²²J. H. Shieh and H. C. Ku, *Chin. J. Phys.* **31**, 1169 (1993).
- ²³C. C. Lai, J. H. Shieh, B. S. Chiou, J. C. Ho, and H. C. Ku, *Phys. Rev. B* **49**, 1499 (1994).
- ²⁴J. C. Ho, C. Y. Wu, C. C. Lai, J. H. Shieh, and H. C. Ku, *Physica B* **194-196**, 203 (1994).